J|A|C|S
ARTICLES
Published on Web 07/10/2007

Toward Quantitative Prediction of Molecular Fluorescence Quantum Efficiency: Role of Duschinsky Rotation

Qian Peng,[†] Yuanping Yi,[†] Zhigang Shuai,*[,†] and Jiushu Shao[‡]

Contribution from the Key Laboratory of Organic Solids, Beijing National Laboratory for Molecular Sciences (BNLMS), Institute of Chemistry, Chinese Academy of Sciences, 100080 Beijing, P. R. China, and Department of Chemistry, Beijing Normal University, 100875 Beijing, P. R. China, State Key Laboratory of Molecular Reaction Dynamics, Institute of Chemistry, Chinese Academy of Sciences, 100080 Beijing, P. R. China

Received November 10, 2006; E-mail: zgshuai@iccas.ac.cn

Abstract: It is a highly desirable but difficult task to predict the molecular fluorescence quantum efficiency from first principles. The molecule in the excited state can undergo spontaneous radiation, conversion of electronic energy to nuclear motion, or chemical reaction. For relatively large molecules, it is impossible to obtain the full potential energy surfaces for the ground state and the excited states to study the excited-state dynamics. We show that, under harmonic approximation by considering the Duschinsky rotation effect, the molecular fluorescence properties can be quantitatively calculated from first principles coupled with our correlation function formalism for the internal conversion. In particular, we have explained the peculiar fluorescence behaviors of two isomeric compounds, *cis*,*cis*-1,2,3,4-tetraphenyl-1,3-butadiene and 1,1,4,4-tetraphenyl-butadiene, the former being nonemissive in solution and strongly emissive in aggregation or at low temperature, and the latter being strongly emissive in solution. The roles of low-frequency phenyl ring twist motions and their Duschinsky mode mixings are found to be crucial, especially to reveal the temperature dependence. As an independent check, we take a look at the well-established photophysics of 1,4-diphenylbutadiene for its three different conformers. Both the calculated radiative and nonradiative rates are in excellent agreement with the available experimental measurements.

1. Introduction

Molecular fluorescence properties are important in chemistry both for applications in materials science (organic light-emitting materials for example[1]) and for biological systems. Luminescence is dictated by the excited-state dynamics, namely, by the competition between radiative decay and the nonadiabatic processes.[2] The nonadiabatic quantum dynamics theory is so far limited to small molecules with 2 or 3 atoms,[3] which is still not practical for molecular design of luminescent materials. The purpose of this contribution is to apply the nonradiative decay rate formalism in the context of correlation function considering the Duschinsky rotation effect[4] to predict the luminescent properties through first-principles calculations for relatively large molecules.

The displaced harmonic oscillator approximation has been widely used, for instance in Marcus theory[5] to describe many different dynamic processes, such as electron transfer and energy transfer in complex systems. However, this approach has assumed that the excited state and the ground state possess the same parabolic potential energy surfaces, except for a rigid displacement in the origins of the normal mode coordinate.[6] Duschinsky rotation effect (DRE) has been found to play an important role in absorption and emission spectra, as seen from the formalism developed by Yan and Mukamel.[7] Pollak and co-workers presented the correlation function formalism of DRE to investigate the excited-state cooling effects for the emission process.[8] It should be pointed out that the correlation function formalism is nontrivial in the sense that it can not only give the analytic formula for harmonic oscillators but also present a framework to include multimode mixing effects and the anharmonicity as well as other complicated quantum dynamics problems.[9] The present work is based on a correlation function formalism of DRE for the internal conversion rate. We will show that a quantitative prediction of molecular luminescent properties

[†] Beijing National Laboratory for Molecular Sciences (BNLMS).
[‡] State Key Laboratory of Molecular Reaction Dynamics.

(1) (a) Tang, C. W.; VanSlyke, S. A. *Appl. Phys. Lett.* **1987**, *51*, 913. (b) Burroughes, J. H.; Bradley, D. D. C.; Brown, A. R.; Marks, R. N.; Mackay, K.; Friend, R. H.; Burns, P. L.; Holmes, A. B. *Nature (London)* **1990**, *347*, 539. (c) Gustafsson, G.; Cao, Y.; Treacy, G. M.; Klavetter, F.; Colaneri, N.; Heeger, A. J. *Nature (London)* **1992**, *357*, 477.
(2) Turro N. J. *Modern Molecular Photochemistry*; Benjamin/Cummings Publishing Co., Inc.: California, 1978.
(3) Aoiz, F. J.; Banares, L.; Castillo, J. F.; Herrero, V. J.; Martinez-Haya, B. *Phys. Chem. Chem. Phys.* **2002**, *4* (18), 4379−4385. Balucani, N.; Casavecchia, P.; Aoiz, F. J.; Banares, L.; Castillo, J. F.; Herrero, V. J. *Mol. Phys.* **2005**, *103* (13), 1703−1714.
(4) Peng, Q.; Yi, Y. P.; Shuai, Z. G.; Shao, J. S. *J. Chem. Phys.* **2007**, *126*, 114302.
(5) Marcus R. A. *J. Chem. Phys.* **1956**, *24*, 966−978, 979−989; *Ann. Rev. Phys. Chem.* **1964**, *15*, 155−196.
(6) Lin, S. H.; Chang, C. H.; Liang, K. K.; Chang, R.; Zhang, J. M.; Yang, T. S.; Hayashi, M.; Shiu, Y. J.; Hsu, F. C. *Adv. Chem. Phys.* **2002**, *121*, 1−88.
(7) Yan, Y. J.; Mukamel, S. *J. Chem. Phys.* **1986**, *85*, 5908.
(8) Ianconescu, R.; Pollak, E. *J. Phys. Chem.* **2004**, *108*, 7778−7784.
(9) Wang, H. B.; Thoss, M. *J. Chem. Phys.* **2003**, *119*, 1289.

can be achieved. Especially, we will point out that considering the DRE is crucial for a correct description of the temperature dependence of luminescence phenomena. The DRE has been taken into account in the studies of optical absorption and emission,[10−13] resonant Raman spectra,[14−16] energy transfer processes,[17−19] and the nonradiative decay[20,21] of small molecules with limited mode mixings. To the best of our knowledge, this work is the first first-principles study on the nonradiative decay for relatively large molecules with unlimited mode mixing. Most importantly, quantitative predictions of the quantum yields both for fluorescence and for internal conversion are demonstrated for several cases. The exotic aggregation induced emission phenomena is explained based on the detailed analysis on the exciton-vibration coupling and the internal conversion.

2. Methodology

We first consider two isomeric compounds, *cis*,*cis*-1,2,3,4-tetraphenyl-1,3-butadiene (compound **1**) and 1,1,4,4-tetraphenyl-butadiene (compound **2**); see Figure 1. Both are excellent light-emitting materials.[22] At room temperature, compound **1** is nonemissive in organic solution, while compound **2** is highly emissive. In addition, compound **1** becomes strongly emissive when lowering the temperature from $T = 300$ to 77 K, or in the solid state,[22] in sharp contrast to the general behavior of solid-state luminescence quenching. This exotic behavior has been termed as "aggregation induced emission" (AIE) and has been found in many luminescent systems.[23] Our previous studies, more qualitative than quantitative, on AIE phenomena concluded that the nonradiative decay rate can be fully suppressed when going from solution phase to solid state, because of the restriction of the side-phenyl ring twisting motion, which consists mostly of low-frequency modes (around 100 cm^{-1}).[24,25] It is important to point out that, in general, low-frequency motions exhibit strong mode mixings, namely, DRE.

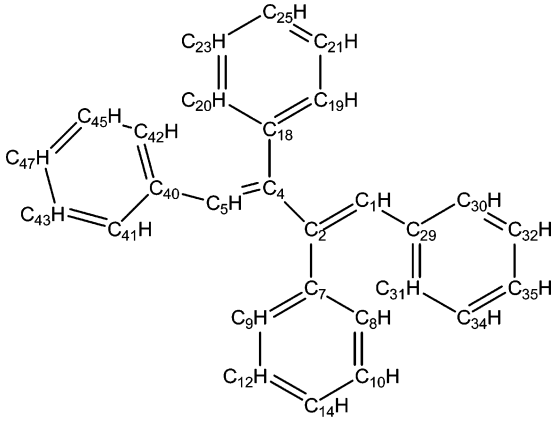

Compound 1

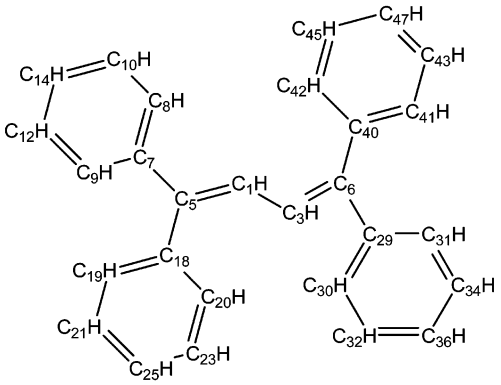

Compound 2

Figure 1. Molecular structures of the two compounds.

The DRE expresses the excited-state vibrational normal mode coordinates as a linear combination of those of the ground state:

$$Q_i^e = \sum_j S_{ij} Q_j^g + D_i \qquad (1)$$

S is called the Duschinsky matrix, and D_i is the i-th normal mode coordinate displacement. A brief description of our new formalism is

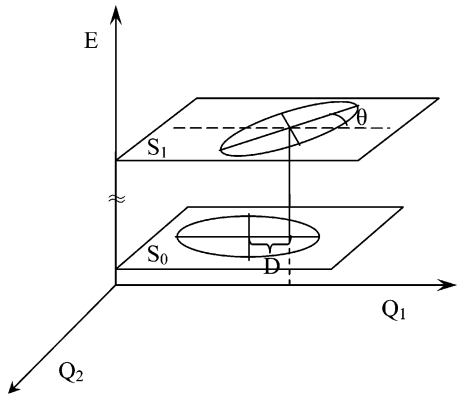

Figure 2. Schematic description of Duschinsky rotation potential energy surface.

(10) (a) Mebel, A. M.; Chen, Y. T.; Lin, S. H. *Chem. Phys. Lett.* **1996**, *258*, 53−62. (b) Mebel, A. M.; Chen, Y. T.; Lin, S. H. *J. Chem. Phys.* **1996**, *105*, 9007−9020. (c) Mebel, A. M.; Lin, S. H.; Chang, C. H. *J. Chem. Phys.* **1997**, *106*, 2612−2620. (d) Mebel, A. M.; Chen, Y. T.; Lin, S. H. *Chem. Phys. Lett.* **1997**, *275*, 19−27. (e) Liao, D. W.; Mebel, A. M.; Hayashi, M.; Shiu, Y. J.; Chen, Y. T.; Lin, S. H. *J. Chem. Phys.* **1999**, *111*, 205−215.
(11) Hemley, R. J.; Lasaga, A. C.; Vaida, V.; Karplus, M. *J. Chem. Phys.* **1988**, *92*, 945−954.
(12) Clauberg, H.; Chen, P. *J. Phys. Chem.* **1992**, *96*, 5676−5678.
(13) Olbrich, G.; Kupka, H. *Z. Naturforsch.* **1983**, *38a*, 937−946.
(14) Hemley, R. J.; Dawson, J. I.; Vaida, V. *J. Chem. Phys.* **1983**, *78*, 2915−2927.
(15) Myers, A. B.; Pranata, K. S. *J. Phys. Chem.* **1989**, *93*, 5079−5087.
(16) Phillips, D. L.; Zgierski, M. Z.; Myers, A. B. *J. Phys. Chem.* **1993**, *97*, 1800−1809.
(17) Lee, E.; Medvedev, E. S.; Stuchebrukhov, A. A. *J. Chem. Phys.* **2000**, *112*, 9015−9024.
(18) Lee, E.; Medvedev, E. S.; Stuchebrukhov, A. A. *J. Phys. Chem. B* **2000**, *104*, 6894−6902.
(19) Sando, G. M.; Spears, K. G.; Hupp, J. T.; Ruhoff, P. T. *J. Phys. Chem. A* **2001**, *105*, 5317−5325.
(20) Mebel, A. M.; Hayashi, M.; Liang, K. K.; Lin, S. H. *J. Phys. Chem. A* **1999**, *103*, 10674−10690.
(21) Hayashi, M.; Mebel, A. M.; Liang, K. K.; Lin, S. H. *J. Chem. Phys.* **1998**, *108*, 2044−2055.
(22) Chen, J. W.; Xu, B.; Ouyang, X. Y.; Tang, B. Z.; Cao, Y. *J. Phys. Chem. A* **2004**, *108*, 7522−7526.
(23) (a) Luo, J.; Xie, Z.; Lam, J. W. Y.; Cheng, L.; Chen, H.; Qiu, C.; Kwok, H. S.; Zhan, X.; Liu, Y.; Zhu, D.; Tang, B. Z. *Chem. Commun.* **2001**, *18*, 1740−1741. (b) Tang, B. Z.; Zhan, X. W.; Yu, G.; Lee, P. P. S.; Liu, Y. Q.; Zhu, D. B. *J. Mater. Chem.* **2001**, *11*, 2974−2978. (c) An, B. K.; Kwon, S. K.; Jung, S. D.; Park, S. Y. *J. Am. Chem. Soc.* **2002**, *124*, 14410−14415. (d) Chen, J. W.; Law, C. C. W.; Lam, J. W. Y.; Dong, Y. P.; Lo, S. M. F.; Williams, I. D.; Zhu, D. B.; Tang, B. Z. *Chem. Mater.* **2003**, *15*, 1535−1546. (e) Chen, J. W. An B. K.; Lee, D. S.; Lee, J. S.; Park, Y. S.; Song, H. S.; Park, S. Y. *J. Am. Chem. Soc.* **2004**, *126*, 10232−10233. (f) Lee, S. H.; Jang, B. B.; Kafafi, Z. H. *J. Am. Chem. Soc.* **2005**, *127*, 9071−9078. (g) Wang, F.; Han, M.; Mya, K. Y.; Wang, Y.; Lai, Y. *J. Am. Chem. Soc.* **2005**, *127*, 10350−10355. (h) Han, M.; Hara, M. *J. Am. Chem. Soc.* **2005**, *127*, 10951−10955.
(24) Yu, G.; Yin, S. W.; Liu, Y. Q.; Chen, J.; Xu, X.; Sun, X.; Ma, D.; Zhan, X.; Peng, Q.; Shuai, Z. G.; Tang, B. Z.; Zhu, D. B.; Fang, W. H.; Luo, Y. *J. Am. Chem. Soc.* **2005**, *127*, 6335−6346.
(25) Yin, S. W.; Peng, Q.; Shuai, Z.; Fang, W. H.; Wang, Y. H.; Luo, Y. *Phys. Rev. B* **2006**, *73*, 205409.

given in the Supporting Information. A schematic representation of DRE is shown in Figure 2.

The photoluminescence efficiency can be expressed as

$$\eta = \frac{k_r}{k_r + k_{nr}} \tag{2}$$

where k_r is the radiative decay rate and k_{nr} is the nonradiative decay rate. The former can be evaluated through the Strickler−Berg (SB) equation[26]

$$k_{r(i0\rightarrow f)} = \frac{64\pi^4}{3hc^3} |\mu|^2 \sum_a \upsilon_{i0\rightarrow fa}{}^3 \, | \int \Theta_{fa}{}^* \Theta_{i0} \, \mathrm{d}Q|^2 \tag{3}$$

where $\upsilon_{i0\rightarrow fa}$ is the frequency of the spontaneous transition from the initial state (usually the first excited state) to the final state (usually the ground state); μ is the electric transition dipole moment between the two states; Θ_{i0} and Θ_{fa} are the vibrational functions for the initial and final states, respectively; h is the Planck constant; and c is the speed of light in vacuum. It is straightforward to show that if there is no displacement for the two electronic states potential energy surface, the SB equation goes exactly to the conventional Einstein spontaneous emission formula, which is valid only for a two-level system.

Here, we consider a system consisting of a collection of harmonic oscillators, that is,

$$\Theta_{l0} = \prod_j \chi_{i0_j}(Q_j), \Theta_{fa} = \prod_j \chi_{fa_j}(Q_j') \tag{4}$$

and use the relations

$$\upsilon_{i0\rightarrow fa} = \upsilon_{if} + \sum_j a_j \upsilon_j \tag{5}$$

$$\text{and } |\langle \chi_{fa_j} | \chi_{i0_j} \rangle|^2 = \frac{S_j^{a_j}}{a_j!} e^{-S_j} \tag{6}$$

We obtain

$$k_{r(i0\rightarrow f)} = \frac{64\pi^4}{h^4 c^3} |\mu|^2 \sum_a (\upsilon_{if} + \sum_j a_j \upsilon_j)^3 \prod_j \frac{S_j^{a_i}}{a_j!} e^{-S_j} \tag{7}$$

S_j is the Huang−Rhys factor for the j-th mode.

In general, there are three major pathways for the nonradiative decay,[2] i.e., (i) internal conversion (k_{IC}) from S_1 to S_0, (ii) an intersystem crossing process (k_{ISC}) from a singlet manifold to a triplet, and (iii) the charge separation (k_{CT}) during the photoisomerization process occurring in the excited state, often assisted by solvent. The luminescence properties are indeed determined by the competition of these k's.

First, we note that both compounds considered in this work are strongly fluorescent at low temperature, which do not show any phosphorescence at $T = 77$ K. For the rigid planar *pi*-conjugated molecules like anthracene, the radiative decay is comparable with intersystem crossing ($\sim 10^7$ s^{-1}), and at low temperature, phosphorescence was observed.[2] In general, for a flexible molecule containing phenyl rings, the internal conversion becomes much faster than the rigid molecules, and the intersystem crossing process cannot compete. We thus do not consider this deactivation process in the nonradiative decay.

Second, we perform a density functional theory (DFT/B3LYP/6-31 g*) to optimize the first excited state (time-dependent DFT formulation) and the ground state geometries, as well as to calculate the oscillator strengths, vibrational normal modes, and transition energies, for the two compounds using the Turbomole package.[27] Previous studies showed that time-dependent DFT methodology is quite accurate for the low-lying excited states even for large molecules.[28] We found that the radiative decay rates are 4.80×10^8 s^{-1} and 3.92×10^8 s^{-1} for compounds **1** and **2**, respectively. As an independent check, our theoretical value for anthracene is calculated to be 3.75×10^7 s^{-1}, which is very close to the experimental value of $\sim 5 \times 10^7$ s^{-1}.[2] This indicates that the radiative decay rate calculated here using the Strickler−Berg formulation is quite reasonable.

Table 1. Bond Length (Å) and Dihedral Angle (deg) Modifications from S_0 to S_1 As Calculated by DFT Approach for the Two Compounds

		S_0	S_1
compound **1**	L (C1−C2)	1.3660	1.4191
	L (C4−C5)	1.3660	1.4198
	L (C4−C2)	1.4872	1.4428
	L (C1−C29)	1.4705	1.4334
	L (C5−C40)	1.4705	1.4330
	L (C2−C7)	1.4984	1.4812
	L (C4−C18)	1.4984	1.4809
	D (C1−C2−C4−C5)	−167.17	−145.42
	D (C2−C1−C29−C31)	21.01	15.73
	D (C1−C2−C7−C9)	70.29	38.01
	D (C5−C4−C18−C20)	70.42	37.77
	D (C4−C5−C40−C42)	20.99	16.63
	L (C1−C5)	1.3687	1.4308
compound **2**	L (C3−C6)	1.3687	1.4310
	L (C4−C2)	1.4463	1.3972
	L (C5−C7)	1.4872	1.4592
	L (C6−C29)	1.4872	1.4592
	L (C5−C18)	1.4950	1.4647
	L (C6−C40)	1.4950	1.4647
	D (C5−C1−C3−C6)	−180.00	−179.22
	D (C1−C5−C7−C8)	−30.52	−23.76
	D (C1−C5−C18−C20)	−58.46	−38.12
	D (C3−C6−C40−C42)	58.43	37.87
	D (C3−C6−C29−C30)	30.53	23.82

It has been well-established that in tetraphenylethylene (TPE), which looks similar in structure to both compounds in Figure 1, the excited-state energy dissipation through ultrafast spectra measurements by Wiersma and collaborators is found to be mainly through torsion-induced charge separation in the excited-state potential energy surfaces, where a conical intersection occurs to convert S_1 to a zwitterionic intermediate state through phenylene twistings.[29] However, we note that compound **2**, which is closer in structure to TPE, is strongly emissive both in solution and in the solid state. This indicates that the k_{CT} pathway should not be the origin of explanation of the exotic luminescence behaviors. We note that, from the calculated k_r's themselves, the difference is not so significant as to decide which compound is emissive or not. Thus we resort to the IC mechanism in this work. As a matter of fact, the flexible molecules like **1** and **2** allow IC much faster than in the case of the rigid ones because the ease of energy dissipation through vibration: in the rigid planar anthracene molecule, the IC process can be completely neglected.[2]

The normal mode displacements and the Duschinsky rotation matrix are calculated using the DUSHIN program developed by Weber, Cai,

(26) Strickler, S. J.; Berg, R. A. *J. Chem. Phys.* **1962**, *37*, 814−822. Brisks, J. B.; Dyson, D. J. *Proc. R. Soc. London, Ser. A* **1963**, *275*, 135−148.

(27) Deglmann, P.; Furche, F.; Ahlrichs, R. *Chem. Phys. Lett.* **2002**, *362*, 511−514. Deglmann, P.; Furche, F. *J. Chem. Phys.* **2002**, *117*, 9535−9538.

(28) Furche, F.; Ahlrichs, R. *J. Chem. Phys* **2002**, *117*, 7433−7447. Rappoport, D.; Furche, F. *J. Chem. Phys.* **2005**, *122*, 064105/1-8. Rappoport, D.; Furche F. *J. Am. Chem. Soc.* **2004**, *126*, 1277−1284. Catalána J.; de Pazb, J. L. G. *J. Chem. Phys.* **2005**, *122*, 244320/1-7. Brause, R.; Krügler, D.; Schmitt, M.; Kleinermannsb, K. *J. Chem. Phys.* **2005**, *123*, 224311/1-11.

(29) Zijlstra, R. W. J.; van Duijnen, P. T.; Feringa, B. L.; Steffen, T.; Duppen, K.; Wiersma, D. A. *J. Phys. Chem. A* **1997**, *101*, 9828−9836. Lenderink, E.; Duppen, K.; Wiersma, D. A. *J. Phys. Chem.* **1995**, *99*, 8972−8977. Ma, J.; Dutt, B.; Waldeck, D. H.; Zimmt, M. B. *J. Am. Chem. Soc.* **1994**, *116*, 10619−10629.

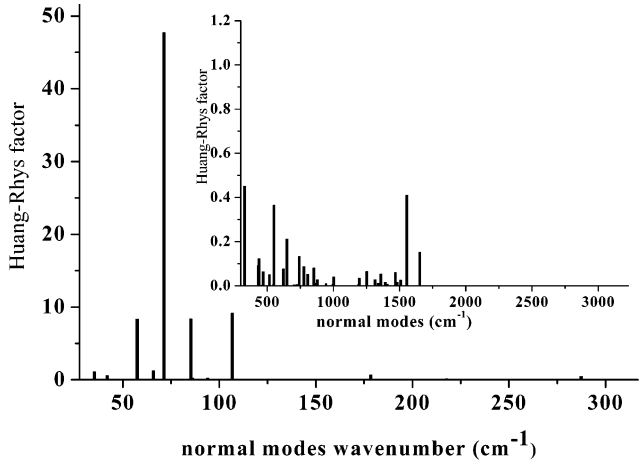

Compound **1**

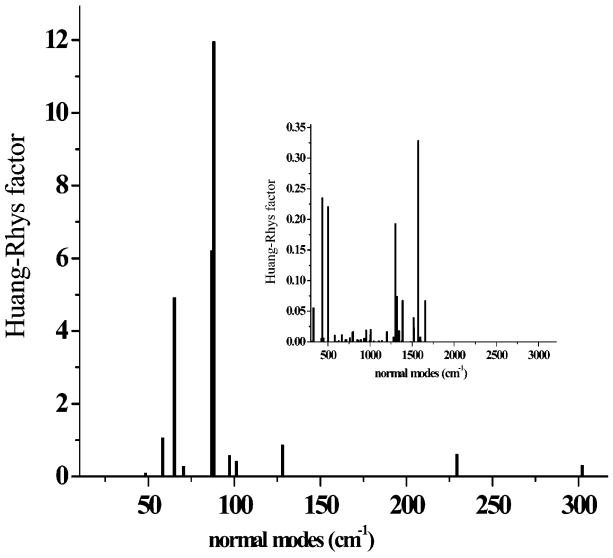

Compound **2**

Figure 3. Calculated Huang−Rhys factors versus the normal mode wave numbers for compounds **1** and **2**.

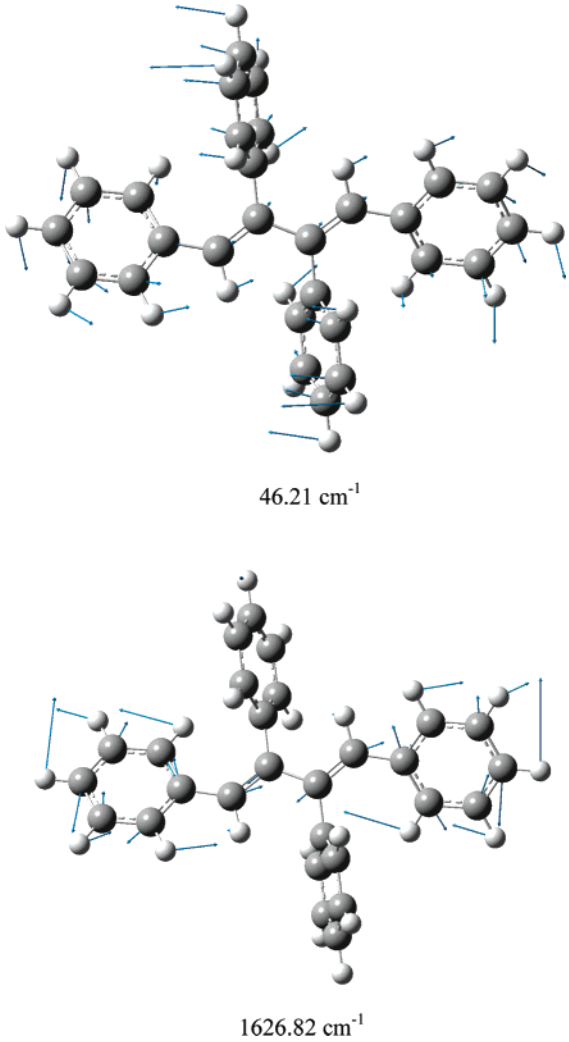

Figure 4. Scheme for the normal mode displacement vectors for vibrations at 46.2 cm^{-1} (side ring twisting) and 1626.8 cm^{-1} (double bond stretching).

and Reimers.[30] The vibronic couplings are calculated at the semiempirical INDO/MRDCI[31] level. Then, the final internal conversion rate from S_1 to S_0 is calculated using the formula given in Supporting Information.[4]

3. Results and Discussion

In Table 1, we give some major geometric modifications upon excitation for the two compounds. From the optimized geometry data of the ground and excited states for the two compounds, two important geometric modifications when going from S_0 to S_1 should be noted: (i) the two mid-phenyls in both compounds are twisted, ca. 30° in compound **1** and ca. 20° for compound **2**; (ii) the main conjugation backbone of butadiene of compound **1** is becoming more nonplanar, with a dihedral angle sharply varying from 167° to 145°, while, for compound **2**, it is planar for both the excited and the ground states. These features tell us that the difference in the potential energy surfaces for the two electronic states should play an important role in the dynamical process. In addition, we find that the steric hindrance between the phenyls at the 2 and 3 sites of butadiene of compound **1** makes the two double bonds not fully planar and decreases the conjugation of the whole molecule, while the butadiene in compound **2** is almost fully planar.

Huang−Rhys (HR) factors characterize the modification of vibrational quanta (absorbed or emitted) when going from one electronic state to another, which are important for determining the internal conversion rate.[24,25] These are calculated according to the quantity D in eq 1, $HR_j = (\omega_j D_j^2)/2\hbar$, and are depicted in Figure 3 for the two compounds. It is clearly seen that (i) the modes with large HR factors (>1.0) all appear at the low-frequency regime for both compounds; (ii) the HR factors in general for compound **1** (with maximum value of 47.7) are much

(30) (a) Weber, P.; Reimers, J. R. *J. Phys. Chem. A* **1999**, *103*, 9830−9841. (b) Cai, Z. L.; Reimers, J. R. *J. Phys. Chem. A* **2000**, *104*, 8389−8408.
(31) (a) Pople, J. A.; Beveridge, D. L.; Dobosh, P. A. *J. Chem. Phys.* **1967**, *47*, 2026−2033. (b) Ridley, J.; Zerner, M. C. *Theor. Chim. Acta* **1973**, *32*, 111−134.
(32) (a) Dahl, K.; Biswas, R.; Maronceli M. *J. Phys. Chem. B* **2003**, *107*, 7838−7853. (b) Velsko, S. P.; Fleming, G. R. *J. Chem. Phys.* **1982**, *76*, 3553−3562. (c) Gehrke, C.; Mohrschladt, R.; Schroeder, J.; Troe, J.; Vohringer, P. *Chem. Phys.* **1991**, *152*, 45−56.
(33) Yee, W. A.; Horwitz, J. S.; Goldbeck, R. A.; Einterz, C. M.; Kliger, D. S. *J. Phys. Chem.* **1983**, *87*, 380−382.
(34) Chattopadhyay, S. K.; Das, P. K.; Hug, G. L. *J. Am. Chem. Soc.* **1982**, *104*, 4507−4514.

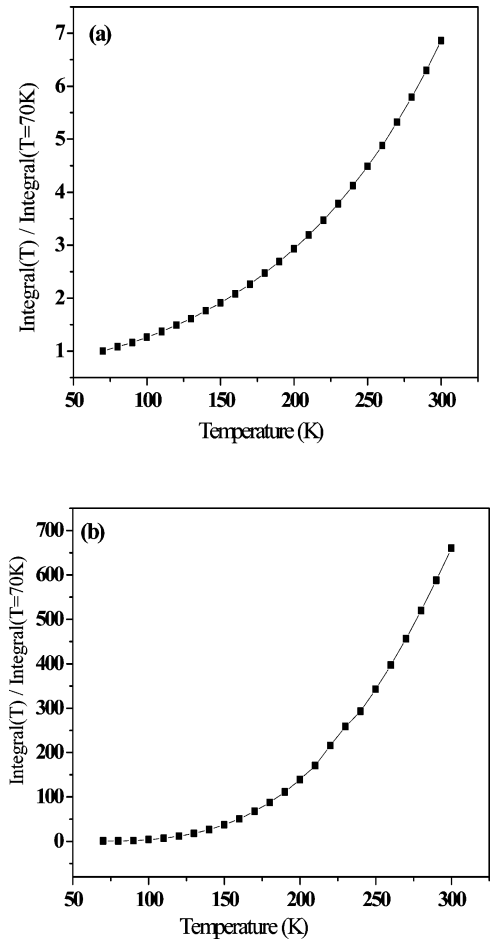

Figure 5. Temperature dependence of internal conversion rate constants of the nonradiative transition from the first excited to ground state of TPBD: (a) without DRE and (b) with DRE.

larger than those for compound **2** (with maximum value of 12); and (iii) the double bond stretching modes at 1626.8 cm^{-1} and 1572.0 cm^{-1} possess HR factors 0.41 and 0.33 for compounds **1** and **2**, respectively. Such features strongly indicate the importance of DRE, because DRE occurs most notably for the low-frequency modes. For the sake of clarity, we show in Figure 4 the normal mode displacement vectors for vibrations at 46.21 cm^{-1} and 1626.82 cm^{-1}, the former being side-ring twisting and the latter being the double-bond stretching.

Selected reorganization energies (>10 cm^{-1}), the corresponding vibrational frequencies, and the displacement for compound **1** and compound **2** are shown in the Supporting Information. The total reorganization energy for the first excited electronic state is 8528 cm^{-1} for compound **1**, and it is 4114 cm^{-1} for compound **2**; the contribution of the low frequency (<100 cm^{-1}) modes to the total reorganization energy is more than 50% in compound **1** and about 37% in compound **2**. There is only one high-frequency mode (double bond stretching mode) with a large reorganization energy in both compounds, 1626.8 cm^{-1} for compound **1** and 1629 cm^{-1} for compound **2**. The nonzero elements of the Duschinsky rotation matrix for low frequency (<100 cm^{-1}) modes for compound **1** are displayed in the Supporting Information. In the IC rate formula, there are two contributions: the electronic coupling and the nuclear motion. Selected values of the electronic part for both compounds are presented in Table 4 in the Supporting Information. Figure 5 shows the calculated temperature dependence of the nuclear part

Table 2. IC Rate Constants (in s^{-1}) from $S_1 \rightarrow S_0$ of Both Compounds at 70 and 300 K[a]

T (K)	compound **1**	compound **2**
70	1.12×10^7	1.26×10^5
	(1.80×10^8)	(2.24×10^5)
300	1.09×10^{10}	1.86×10^6
	(1.23×10^9)	(5.33×10^5)

[a] The values neglecting DRE are given in parentheses. The radiative decay constants are 4.80×10^8 s^{-1} and 3.92×10^8 s^{-1}, respectively, for compound **1** and **2**.

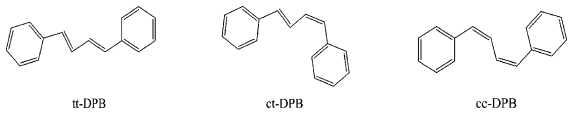

Figure 6. Molecular structures of three DPB conformers.

Table 3. Calculated Radiative and Nonradiative Transition Rates from the First Excited State to the Ground State of DPB at 300 K[d]

	k_r (s^{-1})	k_{nr} (s^{-1})
trans,trans-DPB	9.58×10^8	1.19×10^9
	$(1.4 \times 10^8 - 9.00 \times 10^8)$,[a]	$(0.6 \times 10^9 - 6.2 \times 10^9)$[a]
	$(5 \times 10^8 - 7 \times 10^8)$[b]	$(0.8 \times 10^9 - 1.8 \times 10^9)$[c]
cis,trans-DPB	6.64×10^8	2.84×10^{12}
cis,cis-DPB	7.74×10^8	9.16×10^{11}

[a] Reference 32, measured in a variety of alkane and perfluoroalkane solvents. [b]Reference 33, solvent is 3-methylpentane. [c]Reference 32, solvent is 3-methylpentane. [d]The available experimental data are given in parentheses ranging in different solvents.

of the IC rate of the nonradiative transition $S_1 \rightarrow S_0$ of compound **1** with and without DRE. It can be clearly seen that with DRE, the IC rate increases 700 times from $T = 70$ to 300 K. If DRE is neglected, it goes up approximately 7-fold. We note that, for compound **1**, the photoluminescence peak intensity is indeed enhanced by about 3 orders of magnitude when lowering the temperature from room temperature to 70 K.[20] Thus our results with DRE are in qualitative agreement with experiment. In fact, the IC rate is proportional to the delta-function (energy conservation) weighted Franck−Condon overlap factor between the two electronic states. It is null if there is no normal mode coordinate displacement. Once there is a displacement, the overlap occurs among vibrational states. Since the modes are independent harmonic oscillators, the overlap can only happen within different quantum states of the same mode. The temperature populates the states with larger quanta of vibration, thus increasing the overlap. Once there is a rotation, then in addition to overlaps within the same mode the overlaps start to spread out and to occur between different modes. When temperature is increased, the spread-out effect becomes more and more pronounced due to the vibrational state redistribution to higher quanta and higher frequency modes. This qualitatively explains the more pronounced temperature dependence due to DRE.

The large contribution of the low-frequency modes to the IC rate as in the case of siloles is the major issue in revealing the mechanism for AIE phenomena,[24,25] namely, in the molecular aggregate state. Those low-frequency motions of the side-phenyl rings are hindered, and thus their contributions to the IC rate are strongly suppressed, leaving the radiative decay to be dominant. A complete analysis of the aggregation is beyond the current computational capabilities. However, our results do provide detailed insights for understanding the AIE mechanism.

Table 4. Comparison of Our Calculated and the Experimentally Measured Quantum Yields for DPBs[d]

	tt-DPB	ct-DPB	cc-DPB
fluorescence	0.44	2.34×10^{-4}	8.44×10^{-4}
quantum yield	(0.42)[a]	($<10^{-3}$)[c]	($<10^{-3}$)[c]
intersystem-crossing	NA	NA	NA
quantum yield	(0.02)[b]	(<0.01)[c]	(0.01)[c]
internal conversion	0.56	1.00	1.00
quantum yield	(0.22 + 0.34)[c]	(0.16 + 0.84)[c]	(0.20 + 0.80)[c]

[a] Reference 33. [b]Reference 34. [c]Estimated quantum yields of twisting + internal conversion in ref 35. [d]The experimental data are given in parentheses.

We give in Table 2 the calculated IC rate constants of both compounds at $T = 70$ and 300 K, with and without DRE. It is seen from Table 2 that (i) in compound **1**, there would be no fluorescence at room temperature just because the radiationless rate (1.09×10^{10} s^{-1}) is much larger than the radiative decay rate (4.80×10^{8} s^{-1}); (ii) without considering DRE, it would be concluded that fluorescence could occur for compound **1** at room temperature due to the proximity of the radiationless rate (1.23×10^{9} s^{-1}) to the radiative rate (4.80×10^{8} s^{-1}); (iii) strong fluorescence ($k_{nr} \ll k_r$) is well reproduced for compound **2** in the range of temperature 70−300 K, in good agreement with the experiment. These results indicate that quantitative prediction of molecular fluorescence quantum efficiency can be achieved through first-principles calculation.

To further demonstrate the robustness of the approach and validity of the above conclusion, we then apply our approach to calculate the well-known photophysical properties for 1,4-diphenyl-butadiene (DPB) (see Figure 6) conformers. Tables 3 and 4 present the comparison of our theoretical values with the available experimental results. All the calculations have been performed at the same level as the previous cases. We note that in ref 35, there are two kinds of quantum yields: the internal conversion and the twisting. In the way we calculated the internal conversion rate, all the twisting modes are included in the DRE formalism. Thus we believe that the calculated internal conversion yield can be compared with the sum of the experimental quantum yields of the internal conversion and the twisting in ref 35. The agreement between our theory and the experiment is amazingly good. One point worth noting is that both refs 34 and 35 showed that the intersystem-crossing rate is very low in this system, which fully justifies our assumption in eq 2.

From Tables 3 and 4, it can be seen that both the radiative and internal conversion rates and the quantum yields for the

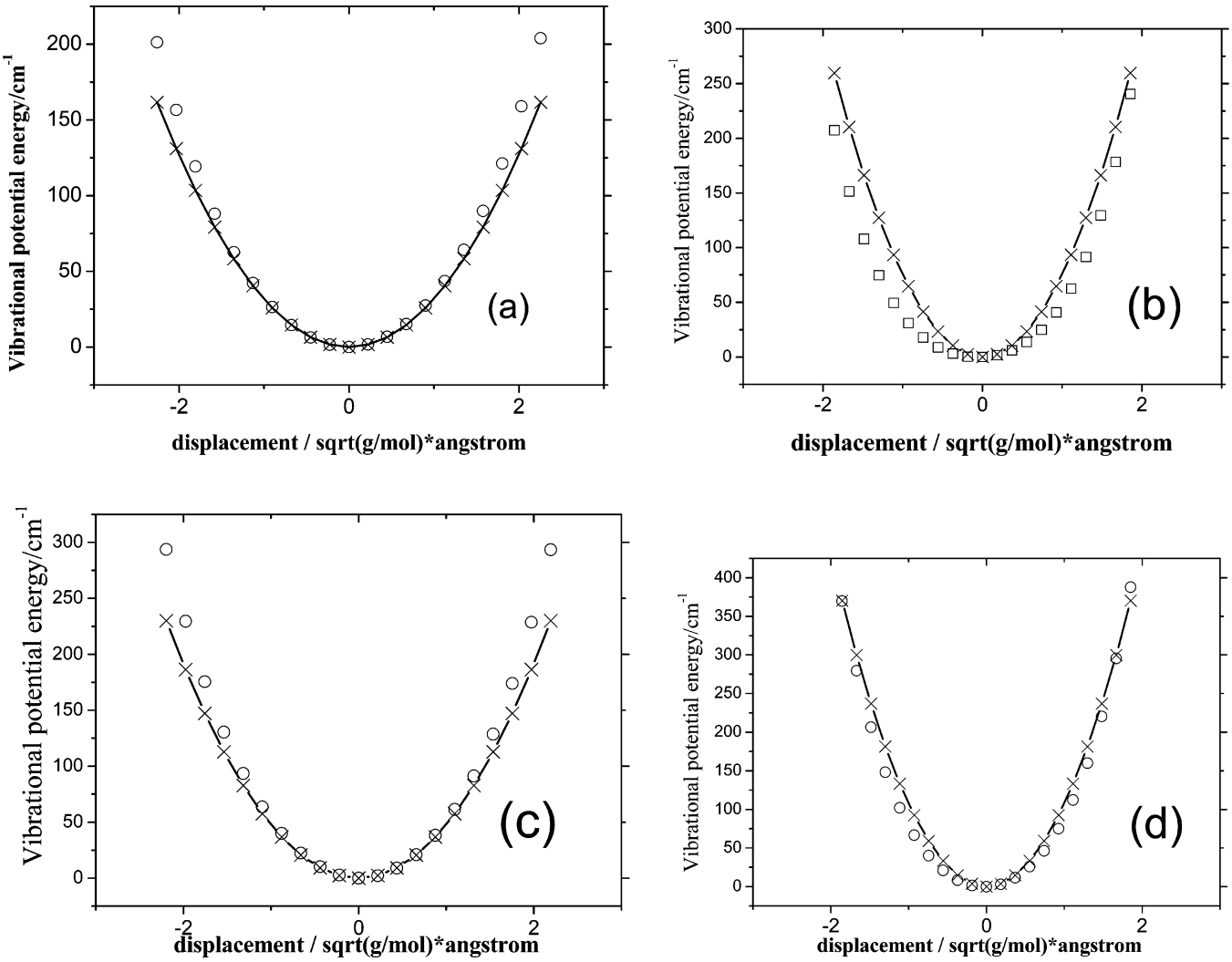

Figure 7. Potential energy surfaces of compound **1** (○) obtained from DFT versus harmonic oscillator (solid line with cross) for the two low-frequency modes. (a) ground state energy versus the fifth mode (46.2 cm^{-1}) coordinate; (b) excited-state energy versus the fifth mode (71.3 cm^{-1}) coordinate; (c) ground state energy versus the sixth mode (56.7 cm^{-1}) coordinate; (d) excited-state energy versus the sixth mode (85.2 cm^{-1}) coordinate.

photophysical processes are in excellent agreement with the existing well-established experiments. In addition, our calculations can fill in the experimental blanks; for instance, the rate values for ct- and cc-DPB are not known to the best of our knowledge. Especially, the different photophysical behaviors of the three conformers can be fully rationalized through our theoretical analysis. We find that, for the three conformers, (i) the radiative transition rates are almost the same and (ii) the internal conversion rate for *trans*,*trans*-DPB is much smaller than those of *cis*,*trans*- and *cis*,*cis*-DPB. The *trans*,*trans*-DPB has a planar ground state geometry and a near-planar excited-state geometry. However, the other isomers have nonplanar geometries in both electronic states. Furthermore, there exist large Huang−Rhys factors for *cis*,*trans*-DPB ($S = 3.6$) and for *cis*,*cis*-DPB ($S = 5.1$), corresponding to the low-frequency rotation of the phenyl ring, while all the Huang−Rhys factors are much smaller ($S < 0.38$) in *trans*,*trans*-DPB. As we pointed out earlier, the rotation of phenyl ring contributes largely to internal conversion processes.

Finally, we caution that even though the difference in the potential energy surface for the ground state and the excited state has been considered in our approach, the harmonicity is still assumed. We illustrate in Figure 7 the comparison between the harmonic oscillator potential and the point-by-point numerical (DFT) calculations for the two important low-frequency modes for TPBD. It is seen that the deviations from the harmonic oscillator are sizable for large normal mode displacements. We note that, for the absorption or emission process, the energy gap between initial and final states can be mediated by the photon energy, which makes the anharmonicity contribution to the Franck−Condon factor much less than that in the present case; namely, the deviations from the minima of surfaces are minor for the former but very remarkable for the latter. The second-order cumulant expansion or the variationally optimized harmonic oscillators[36] can be applied to treat the anharmonicity problem in the present correlation function formalism. However, the fundamental problem here is that we need either exact or approximate potential energy surfaces for both the excited and ground states: for such a big molecule, it is out of the reach of present quantum chemistry theory. Work is in active progress in our group in this direction.

In addition, since the low-frequency contributions are found to be essential, the rotation−vibration coupling which has been neglected in the normal mode calculations might also play a role. Apart from these simplifications, when compared with the commonly applied displaced harmonic oscillator model, this work represented an interesting leap forward. Especially, for the first time, Duschinsky rotation is found to make a big difference in the temperature dependence of the IC process, and the numerical results for TPBDs can well rationalize the exotic photophysical behaviors. Whether the conclusion can survive anharmonicity or rotation−vibration coupling, etc. is an intriguing issue, which deserves further study.

(35) Yee, W. A.; Hug, S. J.; Kliger, D. S. *J. Am. Chem. Soc.* **1988**, *110*, 2164−2169.
(36) Cao, J.; Voth, G. A. *J. Chem. Phys.* **1994**, *102*, 3337−3338.

4. Summary

To summarize, we have applied the correlation function formalism for the nonradiative decay (internal conversion) process from the excited state to the ground state with DRE to quantitatively calculate the molecular fluorescence quantum efficiency. It is found that the inclusion of DRE is crucial to describe the temperature dependence of the IC rate for a relatively large molecule (TPBD) when low-frequency modes are important; that is, we find approximately a 700 times increase in the IC rate when T increases from 70 to 300 K. The peculiarly different fluorescence behaviors for *cis*,*cis*-1,2,3,4-tetraphenyl-1,3-butadiene and 1,1,4,4-tetraphenyl-butadiene have been explained quantitatively. It is found that the low-frequency mode motions for compound **1** contribute largely to the nonradiative decay, in other words, largely dissipate the excited-state energy. These could be easily suppressed by aggregation. When applying our formalism for the known DPB conformers, very nice agreements with experiments have been found for both the rates constants and the quantum yields. This independently confirms the reliability of the quantitatively predictive nature of our approach for molecular fluorescence properties.

Acknowledgment. The authors are indebted to Professor Eli Pollak for illuminating discussions and encouragement, to Professor Jeffrey R. Reimers for providing the DUSHIN program, and to Professor Abraham Nitzan for discussing the anharmonicity, namely, for suggesting the plots of Figure 7. This work is supported by the Ministry of Science and Technology of China through the 973 program (Grant Number 2002CB613406) and the NSFC (Grants 10425420, 20433070, 90503013). The numerical calculations have been done in the supercomputer center of the Chinese Academy of Sciences.

Supporting Information Available: A brief summary of the derivation of our internal-conversion rate formalism, the most important exciton-vibration coupling constants (Huang−Rhys factors), the important Duschinsky rotation matrix elements, and the numerically calculated electronic coupling prefactors for the promoting modes are provided. This material is available free of charge via the Internet at http://pubs.acs.org.

JA067946E